Modeling and Operational Testing of an Isolated Variable Speed PMSG Wind Turbine with Battery Energy Storage

Luminita BAROTE, Corneliu MARINESCU
Transilvania University of Brasov, Brasov, 500024, Romania
luminita.barote@unitbv.ro

***Abstract*—This paper presents the modeling and operational testing of an isolated permanent magnet synchronous generator (PMSG), driven by a small wind turbine with a battery energy storage system during wind speed and load variations. The whole system is initially modeled, including the PMSG, the boost converter and the storage system. The required power for the connected loads can be effectively delivered and supplied by the proposed wind turbine and energy storage systems, subject to an appropriate control method. Energy storage devices are required for power balance and power quality in stand alone wind energy systems. The main purpose is to supply 230 V / 50 Hz domestic appliances through a single-phase inverter. The experimental waveforms, compared to the simulation results, show a good prediction of the electrical variable parameters. Furthermore, it can be seen that the results validate the stability of the supply.**

***Index Terms*—wind energy, SOC, energy storage, stand-alone system.**

I. INTRODUCTION

Many remote communities throughout the world are supplied with electrical energy produced by diesel generators. The rapidly diminishing fossil resources, the rather low reliability of small internal combustion engines (several kW), environmental concerns and the increasing cost of the fuels have motivated the planners to utilize renewable energy sources, such as wind, to replace some or all of the fuel consumed in the autonomous systems. In the case of Wind Energy Conversion Systems (WECS), the interest is also focused on small units, used to provide electricity supply in remote areas that are beyond the reach of an electric power grid or cannot be economically connected to a grid. WECS are the most favored alternatives for supplying electricity in stand-alone situations at this moment due to the fact that wind energy is relatively easily harnessed, wind turbine generators require maintenance which is within reasonable limits and also there is no fuel cost. Wind energy systems have a fluctuating power output due to the wind speed variations, with power output varying by the cube of the wind speed. Integrating an appropriate energy storage system in conjunction with a wind generator removes the fluctuations and maximizes the reliability of power supply [1], [2] at the loads.

Several electrical machines can be used to implement the electromechanical conversion, each of which presents different advantages and disadvantages [3] - [6]. For small power wind system operating in remote and isolated areas, the study of permanent magnet synchronous generators (PMSGs) has been the subject of much research [7], [8]. PMSGs are of special interest in low power wind energy applications due to their small size and high power density. The primary advantage of PMSGs is that they do not require any external excitation current. A major cost benefit in using the PMSG is the fact that a diode bridge rectifier may be used at the generator terminals, since no external excitation current is needed. The system topology used in this article is based on a PMSG connected through a diode bridge rectifier and a boost converter to the DC-link, in small and medium power range [5], [6] installations. Due to the highly variable nature of the wind, the utilization of an energy storage device such as a battery can significantly enhance the reliability of a small stand-alone wind system. Integrating an appropriate energy storage system in conjunction with a wind generator removes the fluctuations and can maximize the reliability of supplying power to the loads [9] - [12].

In the autonomous system, the wind power converter may be operated to maximize the wind energy capture. The captured energy is supplied to the load directly, the difference between the wind power generation and consumer consumption being directed to or supplied by the battery energy storage device connected via the power electronic interface [13]. Lead-acid batteries (LABs) represent an established, mature technology. LABs can be designed for bulk energy storage or for rapid charge/discharge. Improvements in energy density and charging characteristics are still an active research area, with different additions under consideration [14], [15]. Lead-acid batteries are economically the most competitive of long-term energy storage option for most applications requiring large storage capabilities; however, their dynamic response is dependent on many factors: storage capacity, state-of-charge, rate of charge/discharge, temperature, and aging estimation, [16]-[19].

II. STAND-ALONE WIND TURBINE SYSTEM CONFIGURATION

The proposed stand-alone wind energy system, designed for a residential location, is a 2 kW wind turbine (WT) system (Fig. 1) equipped with: i) a direct driven permanent-magnet synchronous generator (PMSG), ii) an AC/DC converter (diode-rectifier bridge + boost converter) for the tracking of the maximum power from the available wind resource, iii) a LAB storage device, iv) an inverter, v) a transformer and vi) resistive loads. It supplies single-phase consumers, at 230 V/50 Hz.

Digital Object Identifier 10.4316/AECE.2012.02014

The wind power is converted into mechanical-rotational energy of the wind turbine rotor. A wind turbine cannot extract the power in the wind completely, theoretical only 59 % of the wind power could be utilized by a WT [20]. However, for the analyzed WT system, the real power coefficient is 0.39. The 2 kW WT block is a Simulink model based on the steady-state power characteristics of the turbine, with base wind speed (= 9 m/s); maximum power at base wind speed (1 p.u of nominal mechanical power); base rotational speed (0.9 p.u of base generator speed) and pitch angle beta equal to zero.

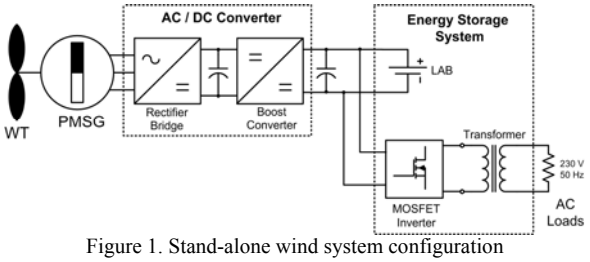

Figure 1. Stand-alone wind system configuration

The wind drives the wind turbine, which is connected to the wind generator; therefore the wind energy is converted into electrical energy. The generator's AC voltage is converted to DC voltage through an AC/DC converter. The rectifier makes the generator AC voltage match the DC voltage, while the boost converter keeps the DC voltage constant. The DC output voltage is fed to the battery bank and also, through an inverter, to the load. The voltage should stay constant for various wind speeds. When the wind speed is too high, the difference in the power supplied by the wind turbine is stored in the battery. When the wind speed is low, the generator, together with the battery bank, can provide sufficient energy to the loads.

The storage system consists of a LAB and a full bridge single-phase inverter that converts the DC voltage of the battery in AC voltage. Further, this voltage is applied to a single-phase transformer, which boosts-up the voltage to 230 V. The inverter controls the power transfer.

A. The PMSG Model

The dynamic model of PMSG is derived from the two-phase synchronous reference frame in which the *q*-axis is 90° ahead of the *d*-axis with respect to the direction of rotation. The electrical model of PMSG in the synchronous reference frame is given by (1) [3], [21] - [23].

$$\begin{cases} \dfrac{di_d}{dt} = -\dfrac{R_a}{L_d} i_d + \omega_e \dfrac{L_q}{L_d} i_q + \dfrac{1}{L_d} v_d \\ \dfrac{di_q}{dt} = -\dfrac{R_a}{L_q} i_q - \omega_e \left(\dfrac{L_d}{L_q} i_d + \dfrac{1}{L_d} \Psi_{PM}\right) + \dfrac{1}{L_q} v_q \end{cases} \quad (1)$$

where subscripts *d* and *q* refer to the physical quantities that have been transformed into the *d-q* synchronous rotating reference frame; R_a is the armature resistance; ω_e is the electrical rotating speed which is related to the mechanical rotating speed of the generator as $\omega_e = n_p \cdot \omega_g$ where n_p is the number of pole pairs; ψ_{PM} is the permanent magnetic flux. Fig. 2 shows the *d*- axis and *q*- axis equipment circuits of PMSG in the *d-q* coordinates that rotate synchronously with an electrical angular velocity [21].

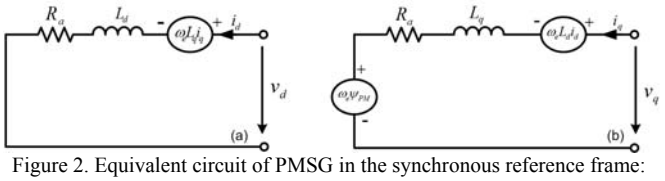

Figure 2. Equivalent circuit of PMSG in the synchronous reference frame: a) d-axis equivalent circuit; b) q –axis equivalent circuit

The electromagnetic torque can be derived from:

$$T_e = 1.5 n_p \cdot [(L_d - L_q) i_d i_q + \psi_{PM} i_q] \quad (2)$$

If the PMSG is taken without rotor saliency (where $L_d = L_q = L$), eq. (1) can be rewritten as:

$$\begin{cases} \dfrac{di_d}{dt} = -\dfrac{R_a}{L} i_d + \omega_e i_q + \dfrac{1}{L} v_d \\ \dfrac{di_q}{dt} = -\dfrac{R_a}{L} i_q - \omega_e \left(i_d + \dfrac{1}{L} \Psi_{PM}\right) + \dfrac{1}{L} v_q \end{cases} \quad (3)$$

and the electromagnetic torque can be regulated by i_q as:

$$T_e = 1.5 n_p \psi_{PM} i_q \quad (4)$$

B. The Boost Converter Model

The unidirectional boost converter constitutes the interface between the battery and the rectifier capacitor and ensures rapid power transfer [24]. The block diagram is shown in Fig. 3 and a simplified model of the boost converter is shown in Fig. 4.

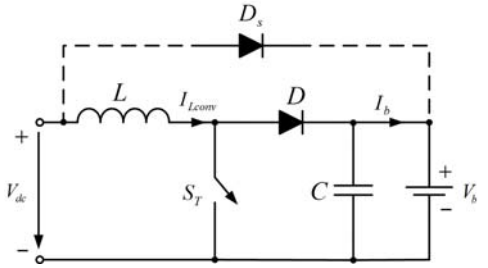

Figure 3. The boost converter diagram

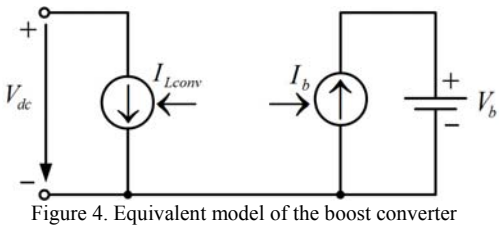

Figure 4. Equivalent model of the boost converter

The voltage relationship between the primary and secondary sides is presented in (5):

$$V_b = \frac{V_{dc}}{1 - D} \quad (5)$$

where *D* is the PWM modulation factor.

When $V_{dc} \geq V_b$ the boost converter is not working and the current provided by the generator is directed through the bypass Schottky diode D_s. In relations (5) and (6) it is assumed that there is no power loss in the converter. The input and output signals of the boost converter are modeled by two controlled current sources (see Fig. 4).

$$I_b = I_{Lconv}(1 - D) \tag{6}$$

Reference current, I^*_{Lconv} is supplied by MPPT regulator. The error between reference current I^*_{Lconv} and measured current I_{Lconv} is applied to a PI regulator. The output of the regulator is summed with the positive voltage reaction, which realizes $1\text{-}V_{dc}/V_b$, the modulation factor D is obtained, which is used as a reference for PWM generator, as shown in Fig. 5. The modulation factor provides the control signal for converter switching device S_T.

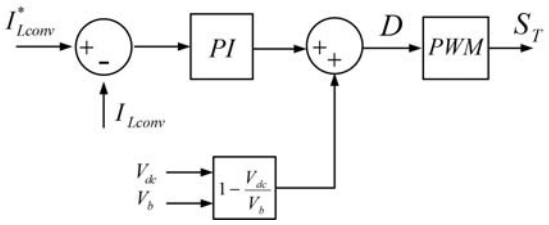

Figure 5. The boost converter control diagram

C. The Maximum Power Point Tracking (MPPT)

To obtain maximum power from a controlled WECS, this has to operate in the variable speed mode. Thus, an adequate controlling method based on Maximum Power Point Tracking (MPPT) is used, in order to maximize the electric output power and to adjust the generator speed [5], [9], [10], [11].

Several studies, including different architectures with associated complexity and implementing different control strategies with associated energy efficiency, have been dedicated to small turbines [25]. Knowledge of the optimal characteristics allows maximizing the energy transfer by controlling the torque, speed, or power. In fact, energy efficiency not only depends on the control strategy but is also influenced by the system topology and its losses [5].

Depending on the wind speed, the MPPT control adjusts the power transferred, bringing the turbine operating points onto the ”maximum power curve”, like in Fig. 6. A PI regulator is used to implement the MPPT function, which provides the reference power for the boost converter, based on wind speed measurements ($v_{p.u}$) and turbine generator speed ($n_{p.u}$). The MPPT control block diagram is shown in Fig. 7.

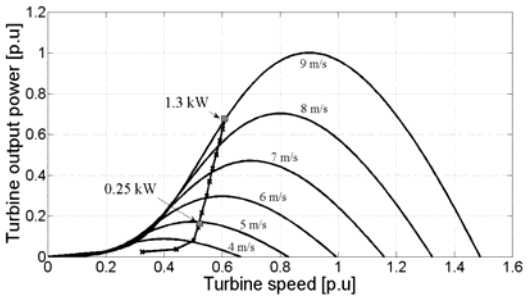

Figure 6. Wind turbine power characteristics

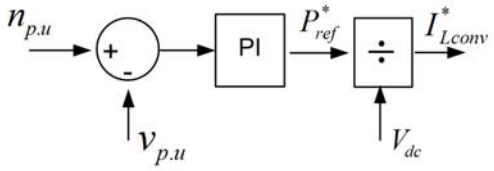

Figure 7. MPPT control block diagram

D. The Energy Storage System

Energy storage system is composed of an inverter and storage element, in this case a bank of LABs (Fig. 8). The battery bank consists of 10 LABs of 12 V each (gel type), connected in series to provide a desired for the inverter battery voltage. The LAB is able to supplement the power provided to the load by the wind turbine when the wind speed is too low.

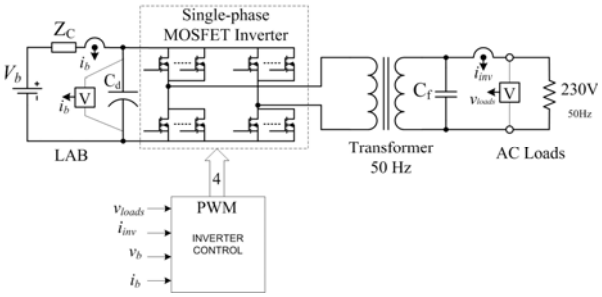

Figure 8. The storage system configuration

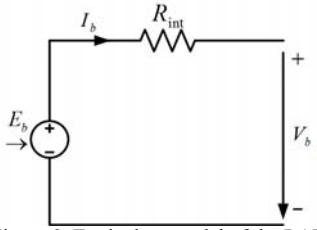

Figure 9. Equivalent model of the LAB

The equivalent scheme of the LAB consists in a controlled voltage source (E_b) in series with the internal resistance (R_{int}) and the LAB voltage (V_b), as shown in the Fig. 9.

It is known that the E_b voltage depends on the charging state, battery type and temperature and is expressed by the following relationship:

$$E_b = E_{b0} - \frac{K \cdot Q}{Q - \int_0^t i_b dt} \tag{7}$$

where: E_{b0} is the battery no load voltage at the rated charge, K is the polarization voltage, Q is the battery capacity and i_b is the battery current. The input of the charging/discharging controller is used as parameter - the SOC (State Of Charge) of LAB, defined as follows [26]:

$$SOC_{[\%]} = SOC_{0[\%]} + \left(\frac{1}{Q_n} \int_0^t i_b dt \right) \cdot 100 \tag{8}$$

where: Q_n is the rated capacity of the LAB.

If the LAB is fully charged, SOC = 1 and if the battery is discharged at the maximum value, SOC = SOC_{min}. For instance, the maximum recommended discharge for LABs used in such applications is 80 %, thus SOC_{min}=0.2. As for LABs is not recommended the full discharge, a SOC_{min}=20 % will be considered in regulator implementation.

The calculation algorithm uses one variable parameter (i_b) and one constant block (Q_n). With a discrete time integrator block, the mathematical operations and an initial SOC value ($SOC_{0[\%]}$), the LAB $SOC_{[\%]}$ is obtained. The SOC block diagram is shown in Fig. 10.

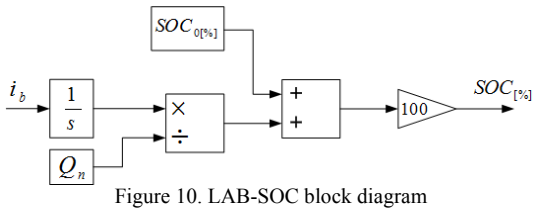

Figure 10. LAB-SOC block diagram

III. Simulation and Experimental Results

The proposed system has been modeled and simulated using the Matlab/Simulink environment [27]. Fig. 11 shows the block diagram. Measurement blocks are also included. The experimental results are obtained via dSPACE on a laboratory test bench, including the described system with a wind turbine emulator that drives the PMSG. The control system is implemented in a dSPACE DS1103 real-time board. This emulator is able to reproduce the steady and dynamic behavior of a real wind turbine.

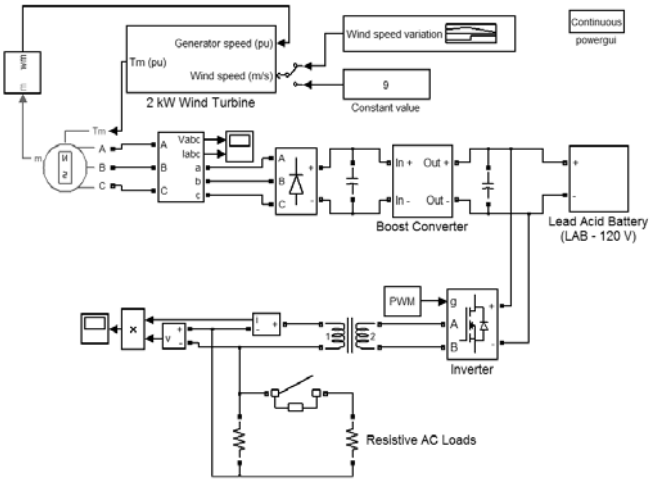

Figure 11. Simulink block diagram

The PMSG has a sinusoidal flux distribution and 8 pairs of poles. Its parameters are listed below:

- Rated power: *2 kW*;
- Rated voltage / frequency: *120 V / 50 Hz*;
- Rated current: *17 A*;
- Rated speed: *400 RPM*;
- Per-phase stator resistance: *2* Ω;
- The d-axis and q-axis stator inductances: $L_d = L_q = 0.001\ H$;
- Flux induced by the magnets in the stator windings: $\psi_{PM} = 0.46\ Wb$.

The hardware scheme is based on a Danfoss VLT - FC302 (5 kW) frequency converter, with vector control/ open loop torque control, and the real-time control system dSPACE DS1103. The operating principle is based on a control loop, where the input signal is the electromagnetic torque of the asynchronous motor (AM), and the output signal is the motor speed. The wind speed can be modified through one independent input of the emulator [28], [29]. The block diagram of the wind turbine emulator is presented in Fig. 12.

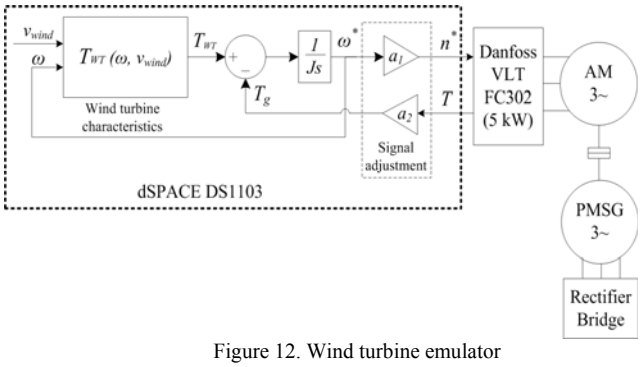

Figure 12. Wind turbine emulator

In order to investigate the system's operation, the following simulations and experiments were carried out:

- Variation of the wind speed, while the load is constant;
- Load switching, with fixed wind speed.

A. Variation of the wind speed, while the load is constant for the following cases:

- **Case 1:** Increasing variation of the wind speed, while the load is constant (P=1 kW);
- **Case 2:** Random variation of the wind speed, while the load is variable.

In **Case 1**, wind speed increases from 5 m/s to 9 m/s. The entire energy load demand is considered 1 kW. The PMSG's electromagnetic torque (Fig. 14) increases with about 60 % when the wind speed starts to increase, while the maximum value of the generator speed is about 230 rpm (Fig. 13). The DC link rectifier bridge voltage value increases with about 2 V in the transient regime (Fig. 15). During this process, the LAB voltage increases by about 2 V (Fig. 16). When $I_{LAB} > 0$, the battery is charging, and when $I_{LAB} < 0$ the battery is discharging.

As it can be seen in Fig. 17, at a wind speed of 5 m/s, the power produced by the wind turbine (approximately 0.3 kW, see Fig. 19a,b) cannot supply the entire load energy demand (1 kW), therefore the battery will supply the difference. The initial LAB SOC is considered 78.92 %. In the transient regime, the battery SOC decreases in order to ensure the stability of the supply for the loads (Fig. 18).

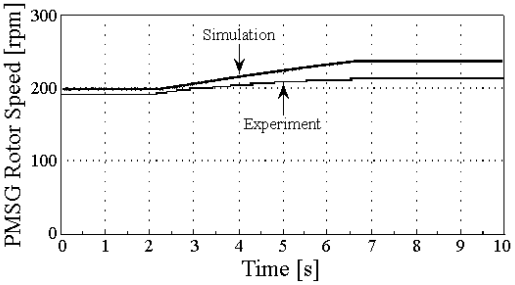

Figure 13. The PMSG rotor speed variation

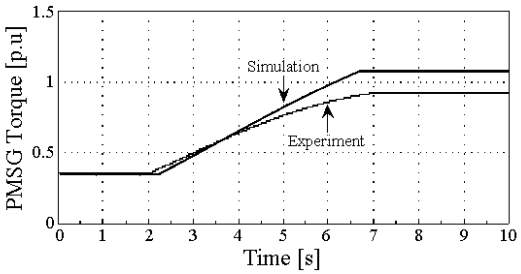

Figure 14. The PMSG electromagnetic torque

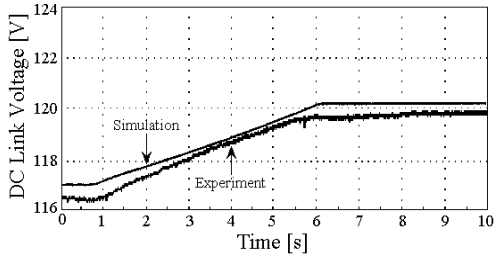

Figure 15. The DC link rectifier bridge voltage variation

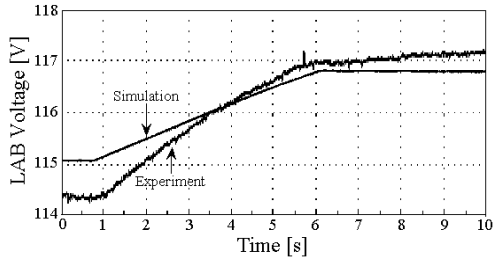

Figure 16. The LAB voltage variation

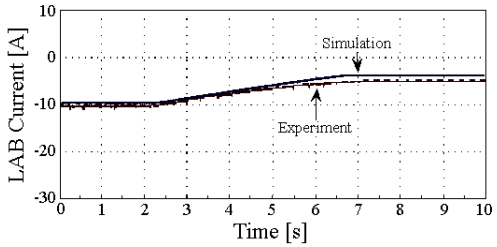

Figure 17. The LAB current variation

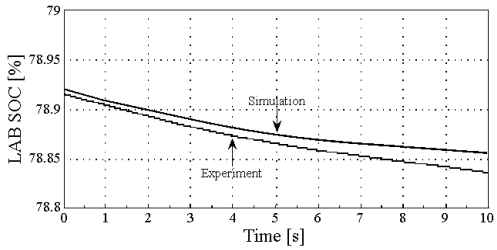

Figure 18. The LAB-SOC variation

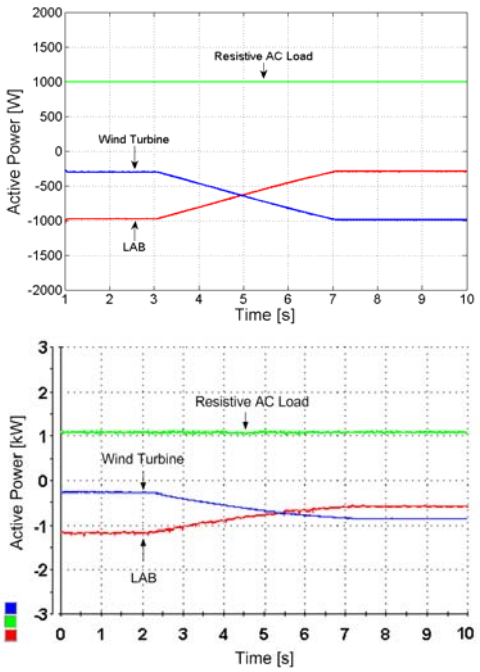

Figure. 19. The active power balance of the system:
(a) Simulation results; (b) Experimental results.

In the **Case 2**, a typical wind profile is implemented, within 100 seconds, as shown in Fig. 20. The profile is based on real wind data characteristics [30]. In a wind-storage system, the battery acts to smoothen out the output power of the wind turbine by charging and discharging accordingly. Corresponding to the two load values which are connected and disconnected under waveform of Fig. 27, the experimental results are summarized in Figs. 21 - 27.

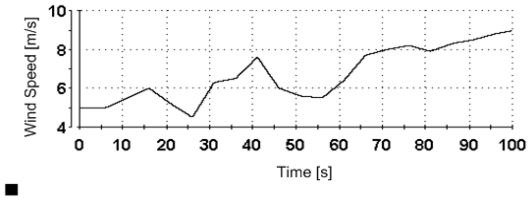

Figure 20. Typical wind profile for storage device

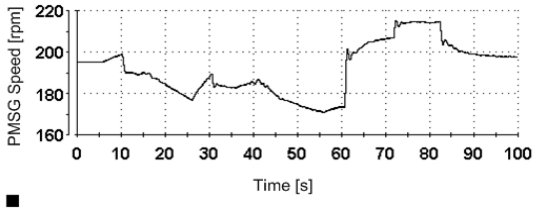

Figure 21. The PMSG rotor speed variation

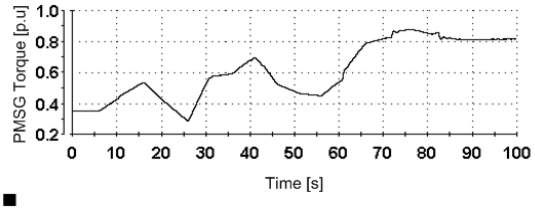

Figure 22. The PMSG electromagnetic torque

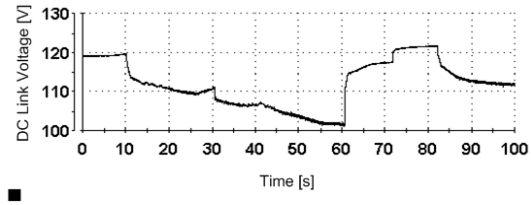

Figure 23. The DC link rectifier bridge voltage variation

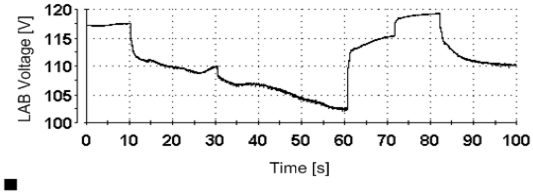

Figure 24. The LAB voltage variation

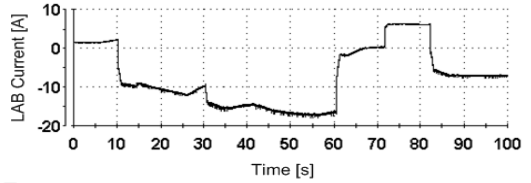

Figure 25. The LAB current variation

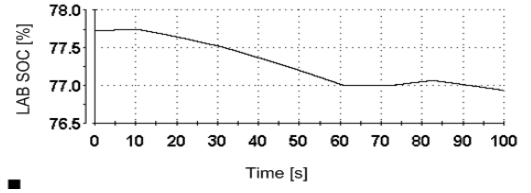

Figure 26. The LAB-SOC variation

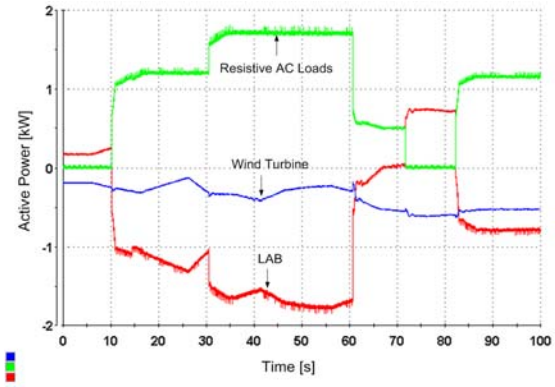

Figure 27. The active power balance of the system

B. Load switching, with fixed wind speed for the following cases:

- **Case 1:** 2 kW load switching at 0 m/s;
- **Case 2:** 1 kW load switching at 9 m/s.

In **Case 1**, the wind turbine doesn't work (v = 0 m/s). At t=1.5 s, a 2 kW load is connected and then subsequently disconnected at approx. t=5.2 s.

During the transient event, the LAB voltage decreases with approximately 8 V (Fig. 28), and the negative current implies that the LAB has gone into the discharge mode in order to ensure the stability of the supply for the loads (Figs. 29 and 30). Fig. 31 shows that the active power balance of the system is maintained regardless of the load change.

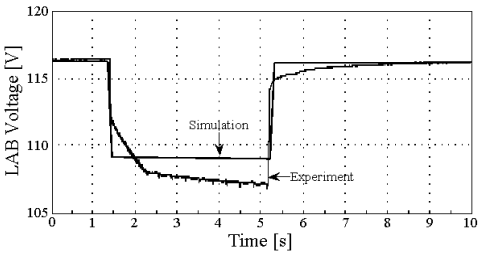

Figure 28. The LAB voltage variation

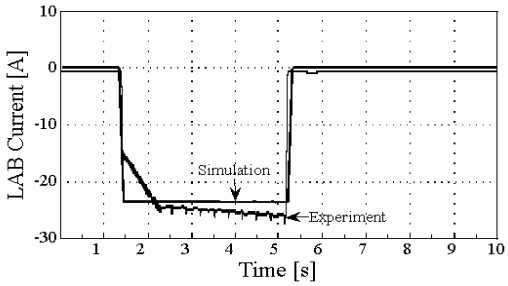

Figure 29. The LAB current variation

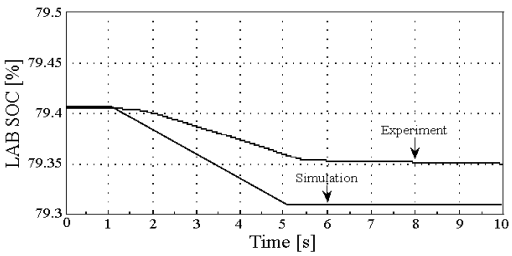

Figure 30. The LAB-SOC variation

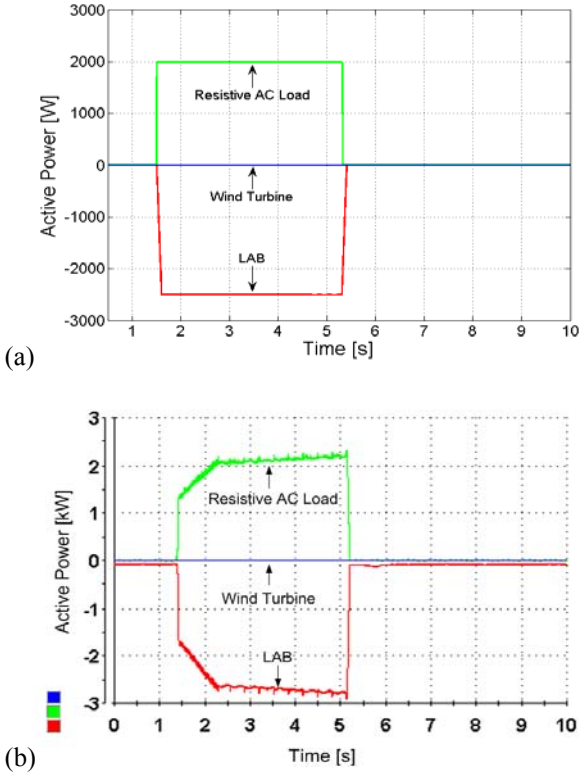

Figure 31. The active power balance of the system: (a) Simulation results; (b) Experimental results.

Also, when the wind turbine doesn't work (v = 0 m/s) and at t=1.5 s a RL load (2 kW/1 kvar) is connected and then subsequently disconnected at approx. t=5s, the power balance into the analyzed configuration is presented in Fig. 32.

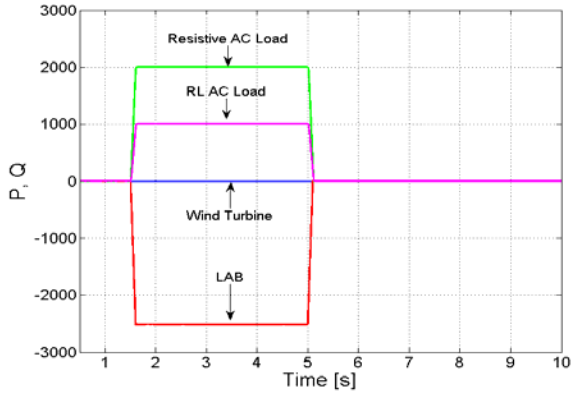

Fig. 32. The power balance of the system with RL loads

As one can see from the new introduced simulation there is no effect of the L component on the dc side power circulation, so to study especially the RL case is of no interest. Only the inverter has to be oversized to bear the reactive component.

In **Case 2**, the wind speed is maintained constant at 9 m/s. At t=0.5 s, a 1 kW load is connected and then subsequently disconnected at t=5 s. The simulation and experimental results for wind turbine emulator are summarized in Figs. 33, 34, whereas the DC link rectifier bridge voltage variation is presented in Fig. 35.

Figs. 36 and 37 demonstrate that the LAB operating mode changes from charge to discharge during the transient event. Because initially no load is connected, the power

difference supplied by the wind turbine is stored in the battery. The LAB stored energy is released when the 1 kW load is connected, thus the load supply being ensured. The SOC slope changes when the load is switched on and off, as shown in Fig. 38, which means that the battery passes from charging to discharging mode. Consequently, Fig. 39 shows that the active power balance of the system is maintained with the LAB, which will switch from the charging to the discharging mode.

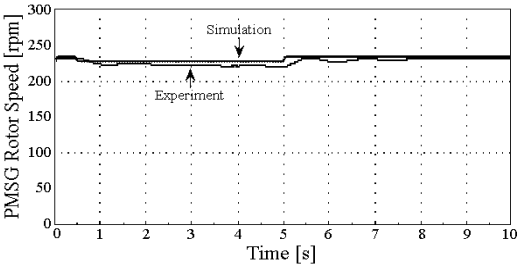

Figure 33. The PMSG rotor speed variation

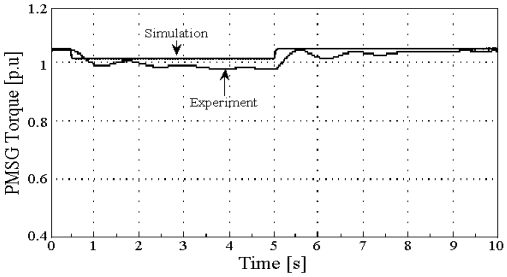

Figure 34. The PMSG electromagnetic torque

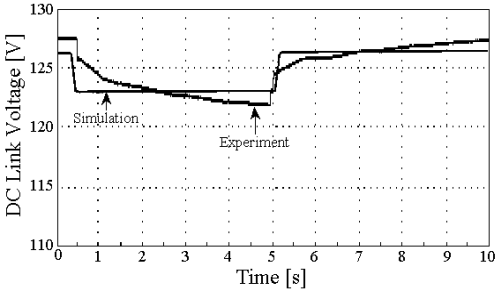

Figure 35. The DC link rectifier bridge voltage variation

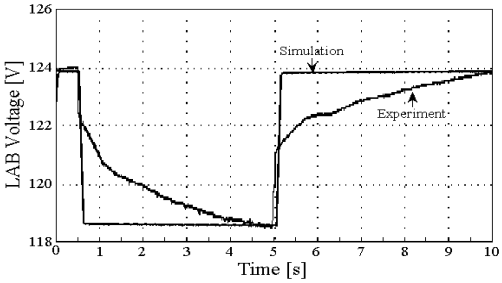

Figure 36. The LAB voltage variation

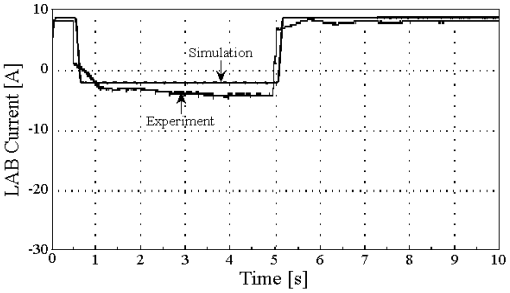

Figure 37. The LAB current variation

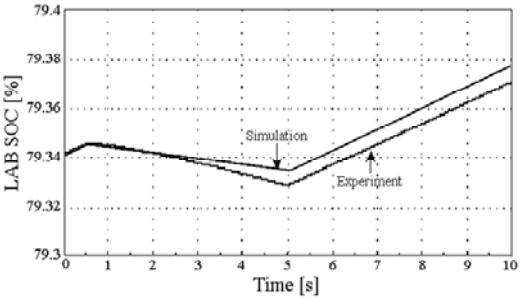

Figure 38. The LAB-SOC variation

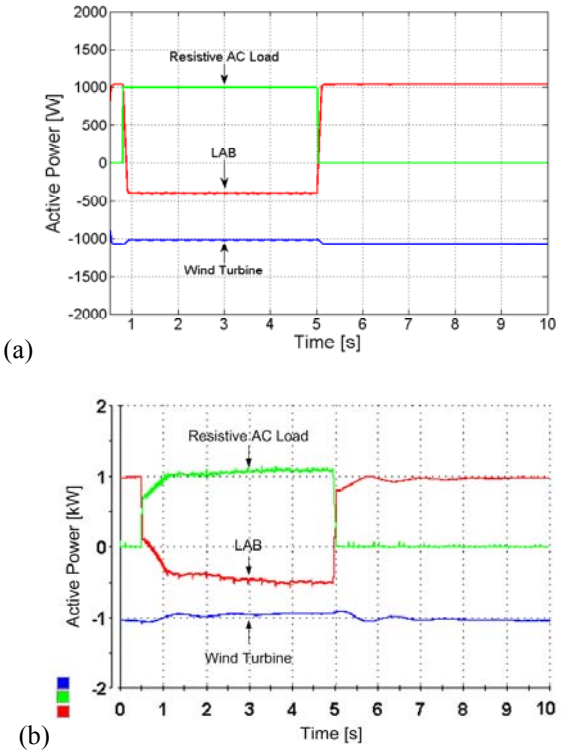

Figure 39. The active power balance of the system: (a) Simulation results; (b) Experimental results.

By following the experimental results, it can be observed that small changes are reflected in the waveforms of the voltage and the current through the battery. The explanation for these differences is that the real system is more complex than the model used in simulation and hence its performance can be affected by a few other parameters that are not considered in the simulation (the neglected/unknown wires, etc.). These differences are more significant in the results presented for load switching, for example in Fig. 36). This fact is due to the real inverter used in the laboratory test bench, which has low dynamics during the transient regime, compared with the simulation case, where an ideal inverter is modeled.

In addition, the mismatch of the time axis between simulation and experimental results occurs because of the difficulty of controlling the real system start time, as opposed to the simulation case.

IV. Conclusions

This paper presents a variable speed PMSG wind turbine system, which is modeled, analyzed and verified. The system includes an associated battery energy storage system, used to stabilize the output voltage for autonomous applications. The MPPT algorithm, which controls the

power electronic interface, will ensure a maximum extraction of energy from the available wind. LAB always ensures the safe supply of the loads (households), regardless of the problems caused by wind speed or loads variations, by switching between the charging and the discharging mode.

The main original contributions of this paper are related to the conceptual design and development of a control topology which achieves MPPT, voltage monitoring and battery SOC with optimal conditions for battery charging.

The work carried out also achieved the design and implementation of a wind turbine emulator with an induction motor and a frequency converter. The experimental laboratory test bench developed has enabled a practical validation of the model and the simulation results through direct testing.

The both simulation and experimental results show clearly that the active power balance of the system is being satisfied during transient loads and variable wind speed conditions. Thus, through the analysis performed and the case studies considered, it can be concluded that the proposed system is able to effectively provide reliable and good quality power to the customers in autonomous power systems.

The work performed and results obtained also highlight the functionality and efficiency of the control system developed and offer perspectives for future research on autonomous wind energy system control strategies.

As a positive aspect is that in the developed autonomous structure with PMSG, operating under variable speed, were integrated different types of storage devices, such as Vanadium Redox Battery [31] and Lithium Ion Battery [32], but experimental measurements were performed only for LAB.

Future works will take into account the energetically aspect of the losses which were not optimally considered in this work regarding to the generator (the system) rated power; the system losses (friction, magnetizing currents, converter losses) being close to the nominal ones are disproportionately large compared with operating power (see Fig. 31a,b).

ACKNOWLEDGMENT

This paper is supported by the Sectoral Operational Programme Human Resources Development (SOP HRD), financed from the European Social Fund and by the Romanian Government under the project number POSDRU/89/1.5/S/59323.

REFERENCES

[1] G. Iwanski, W. Koczara, "Autonomous power system for island or grid-connected wind turbines in distributed generation", European Transactions on Electrical Power, vol. 18, pp. 658-673, 2008.

[2] B. Sorensen, *Renewable Energy - Third Edition*, Elsevier Academic Press, UK, 2004.

[3] N. D. Caliao, "Small-signal analysis of a fully rated converter wind turbine", J. Renewable Sustainable Energy, vol. 3, 2011.

[4] G. Michalke, A. D. Hansen, "Modelling and control of variable speed wind turbines for power system studies", Wind energy, vol. 13, 2010.

[5] A. Jamal, et al., "A review of power converter topologies for wind generators", Journal of Renewable Energy, vol. 32, pp. 2369-238, 2007.

[6] M. Adam, et al., "Architecture Complexity and Energy Efficiency of Small Wind Turbines", IEEE Trans. Ind. Electron., vol. 54, pp. 660-670, 2007.

[7] T. Tudorache, M. Popescu, "Optimal Design Solutions for Permanent Magnet Synchronous Machines", Advances in Electrical and Computer Engineering Journal, vol. 11, no. 4, pp.77 – 82, 2011.

[8] Y. Oner, N. Bekiroglu, S. Ozcira, "Dynamic Analysis of Permanent Magnet Synchronous Generator with Power Electronics", Advances in Electrical and Computer Engineering Journal, vol. 10, no. 2, pp. 11 – 15, 2010.

[9] L. Barote, C. Marinescu, "Storage Analysis for Stand-Alone Wind Energy Applications", Proc. of IEEE OPTIM 2010, Brasov, Romania, pp. 1180 – 1185.

[10] L. Barote, C. Marinescu, „PMSG Wind Turbine System for Residential Applications", Proc. of IEEE International Symposium on Power Electronics, Electrical Drives, Automation and Motion, SPEEDAM 2010, 14-16 June, Pisa, Italy, 2010, pp. 772 – 777.

[11] L. Barote, et al., "Stand-Alone Wind System with Vanadium Redox Battery Energy Storage", Proc. IEEE OPTIM 2008, Brasov, Romania, pp. 407 – 412.

[12] B. Fleck, M. Huot, "Comparative life-cycle assessment of a small wind turbine for residential off-grid use", Journal of Renewable Energy, vol. 34, pp. 2688-2696, 2009.

[13] C. Liu, et al., "An efficient wind-photovoltaic hybrid generation system using doubly excited permanent magnet brushless dc machine", IEEE Trans. Ind. Electron. vol. 57, pp. 831-839, 2010.

[14] M. J. Vasallo, et al., "A Methodology for Sizing Backup Fuel-Cell/Battery Hybrid Power Systems", IEEE Trans. Ind. Electron. vol. 57, pp.1964-1975, 2010.

[15] M. Swierczynski, et al., "Overview of the Energy Storage Systems for Wind Power Integration Enhancement", Proc. IEEE ISIE 2010, Poland, Gdansk, pp. 3749 – 3756.

[16] Y. H. Sun, et al., "Aging Estimation Method for Lead-Acid Battery, IEEE Trans. on Energy Conversion", vol. 26, pp. 264-271, 2011.

[17] S. M. Lukic, et al., "Energy storage systems for automotive applications", IEEE Trans. Ind. Electron. vol. 55, 2258-2267, 2008.

[18] Y. Chang, "Lead-acid battery use in the development of renewable energy systems in China", Journal of Power Sources, vol. 191, pp. 176–183, 2009.

[19] C. Abbey, et al., "A Knowledge-Based Approach for Control of Two-Level Energy Storage for Wind Energy Systems", IEEE Trans. on Energy Conversion, vol. 24, pp. 539-547, 2009.

[20] T. Ackermann, *Wind Power in Power Systems,* John Wiley & Sons Ltd. England, 2005.

[21] Y. Ming, et al., "Modeling of the Wind Turbine with a Permanent Magnet Synchronous Generator for Integration", IEEE Power Eng. Society General Meeting, 2007.

[22] I. Boldea, *Variable Speed Generators–The Electric Generators Handbook*, CRC Press. USA, 2006.

[23] L. G. Gonzalez, et al., "Synchronization Techniques Comparison for Sensorless Control Applied to PMSG", Proc. of ICREPQ'09, Spain, 2009.

[24] C. Sreekumar, V. Agarwal, "A hybrid control algorithm for voltage regulation in dc–dc boost converter", IEEE Trans. Ind. Electron., vol. 55, no. 6, pp. 2530–2538, Jun. 2008.

[25] F. Blaabjerg, Z. Chen, *Power Electronics for Modern Wind Turbines*, Morgan & Claypool Publishers, USA, 2006.

[26] P. Thounthong, et al., "Control Algorithm of Fuel Cell and Batteries for Distributed Generation System", IEEE Trans. Energy Conversion vol. 23, pp. 148 -155, 2008.

[27] SimPowerSystems, www.mathworks.com.

[28] L. A. C. Lopes, et al., "A Wind Turbine Emulator that Represents the Dynamics of the Wind Turbine Rotor and Drive Train", Proc. of IEEE Power Electronics Specialists Conference, 2005, pp. 2092 – 2097.

[29] T. Tudorache, V. Bostan, "Wind Generators Test Bench. Optimal Design of PI Controller", Advances in Electrical and Computer Engineering Journal, vol. 11, no. 3, pp.65 – 70, 2011.

[30] Renewable energy system design tools - Historical weather and climate data for Sulina: http://www.energymatters.com.au/climate-data/?q=sulina&find=Search.

[31] L. Barote, et al., "VRB Modelling for Storage in Stand-Alone Wind Energy Systems", Proc. of IEEE PowerTech Conference, pp. 1078-1083, 2009.

[32] L. Barote, C. Marinescu, "Li-Ion Modeling for Storage in Stand-Alone Wind Energy Systems", Proc. of SIELMEN'09, pp. 347-353. 2009.